MOLECULAR DYNAMICS SIMULATION OF WATER*

ALFONS GEIGER
Physikalische Chemie, Universität Dortmund
D-4600 Dortmund, GERMANY

1. Introduction

Two decades of computer simulation studies on water and aqueous solutions have immensely broadened our knowledge about this ubiquitous but nonetheless unusual liquid. Perhaps most remarkable is the fact that it is now possible to reproduce, in a molecular dynamics (MD) simulation, a wide range of measurable properties of water, from thermodynamics to structure and microdynamics, particularly most—if not all—of its numerous 'anomalies'. This confirms that the MD simulations reproduce 'real water' and encourages one to use the simulations to examine features that are not directly measurable, but of central importance for the understanding of water, like the hydrogen bond network.

2. Interaction Models

A typical molecular dynamics (MD) simulation consists of solving Newton's equations for a system of N particles given their initial positions, velocities, and an interaction potential[1]. Having obtained the force on each particle for the molecular configuration, the new positions and velocities may thus be calculated. Since the actual computer program solves these equations by numerical integration, a finite time step, typically $\sim 10^{-15}$s, is required. The final result of a simulation is therefore a time history of configurations each separated by this time Δt.

Given a numerical integration algorithm, the most important component of any MD simulation is the choice of the potential energy function u, which in general is an explicit function of the positions of every molecule $\vec{x}_i$ (more generally, of positions and orientations). The configurational energy u can be expanded as an explicit sum of 2-body, 3-body,...,n-body interactions:

$$u(\vec{x}_1,\ldots,\vec{x}_n) = \sum_{i<j}^{N} V_2(\vec{x}_i,\vec{x}_j) + \sum_{i<j<k} V_3(\vec{x}_i,\vec{x}_j,\vec{x}_k) + \ldots$$

In theory we would prefer to use as many terms of this expansion as possible, but limitations on computational ability typically force one to use one of the following approaches, most of which involve approximating u by a sum over 2-body potentials $V_2(\vec{x}_i,\vec{x}_j)$ between particles i and j [2].

* Lecture notes prepared by Sharon Glotzer and Peter H. Poole.

H. E. Stanley and N. Ostrowsky (eds.), Correlations and Connectivity, 198–213.

One approach is to use a "pure pair potential" in which 3-body and higher interactions are explicitly dropped. The remaining 2-body interaction V_2 can be calculated *ab initio* from a quantum mechanical consideration of the "supermolecule" consisting of an isolated pair of water molecules. The pair interaction energy is determined for a large (~ 200) set of relative positions and orientations of this water dimer. The result is a set of particular values for V_2 in the space of the dimer's relative coordinates which are then fitted to some analytical function. This function is chosen as the best compromise between mathematical simplicity and numerical accuracy, and becomes the potential energy surface for the dimer. An example of a pure pair potential is the MCY potential of Clementi et al. [3].

An alternative approach is to include the 3-body and higher-order interactions via an "effective pair potential" which is explicitly a 2-body potential but includes parameters which are adjusted so that the results of a simulation concur with known experimental results . The prototype of this class of models is the ST2-potential of Rahman and Stillinger [4].

A typical effective pair potential consists of a Lennard-Jones center surrounded by some configuration of point charges. For example, the very simple SPC potential of Berendsen et al.[5] takes the following form:

$$V_2(\vec{x}_i,\vec{x}_j) = 4\epsilon\left\{\left(\frac{\sigma}{r_{OO}}\right)^{12} - \left(\frac{\sigma}{r_{OO}}\right)^{6}\right\} + \sum_{\alpha,\beta}\frac{q_\alpha q_\beta}{r_{\alpha\beta}}.$$

Here the Lennard-Jones parameters ϵ and σ, as well as the partial charges q_α, which are positioned at the atomic nuclei, are the adjustable parameters. They were fitted so that the results of the simulation agreed with experimental thermodynamic data for water at 300 K and 1.0 g/cm^3. The adjusted parameters yield a dipole moment of the individual molecules and a potential well depth of the water dimer which are both increased compared to the experimental gas phase values. This demonstrates the influence of the many body effects.

If no internal degrees of freedom are considered, the result is a rigid effective pair potential, of which there are many realizations [2]. Flexible effective pair potentials are those that include intramolecular potential terms in order to simulate internal vibrations [6]. Such models are used to obtain simulation results for spectroscopic studies of water.

The third important class of potentials represent *polarizable* water molecules. All the rigid models described above have a fixed dipole moment; however *induced* dipole moments in the condensed phase make an important contribution to the intermolecular interactions. Hence polarizable models explicitly allow for the total dipole moment of a water molecule to change in response to its molecular environment. This is typically achieved in one of two ways. One can calculate the *induced* part of the dipole moment in the liquid $\vec{\mu}_{\rm ind}$, using the (approximately isotropic) polarizability of the gas phase α_0, and the electric field $\vec{E}_{\rm loc}$ experienced by the

molecule:

$$\vec{\mu}_{\rm ind} = \alpha_0 \vec{E}_{\rm loc}.$$

However the effect of $\vec{\mu}_{\rm ind}$ on neighboring dipoles—and hence on $\vec{E}_{\rm loc}$—must be included. This means that $\vec{E}_{\rm loc}$, and $\vec{\mu}_{\rm ind}$, should be calculated iteratively until a stable result is obtained. In practice, this is usually possible within only a few steps, but this is substantial since the overall computation time increases proportionately[7]. The other way to obtain a polarizable model involves including strategically placed variable point charges with the rigid fixed-site charges. The change of position or magnitude of these charges in response to Coulombic forces from other molecules changes the molecule's dipole moment [8].

There exists a need for realistic water models which explicitly incorporate many body terms, because the effective pair potentials described above have their adjustable parameter optimized to correspond to one particular state point (fixed T, ρ) of the bulk liquid. This means that simulations carried out with such a model under other conditions will be subject to errors dependent on how strong the state dependence of the adjustable parameters is. If polarizable water models incorporate non-pairwise additive interactions correctly, such models have greater promise to simulate the full range of water states reliably; ideally, the same model could be used to simulate both gaseous and condensed phases [9], as well as heterogeneous systems in which water is in the presence of ions or confining surfaces, near which we can expect water properties to be significantly different than in the bulk.

Comparison with Experiments

MD simulations of liquid water using a variety of potentials have been made. It turns out that several potentials are able to reproduce a wide range of properties, but that none of them simultaneously reproduces all of the properties with comparable accuracy. The widely used SPC potential, e.g., reproduces fundamental thermodynamic properties like density and internal energy within about three percent, while the first derivative quantities—like heat capacity and compressibility—are reproduced within about 40 percent. In a number of papers detailed comparisons between different model potentials are made[10,11].

In Fig. 1 are compared the three experimental partial pair correlation functions for water, and those calculated from MD simulations[12]. It is interesting to note how successfully the liquid structure is reproduced from several independent water models. In fact, one may say that any reasonable approach that incorporates the high directionality of intermolecular interactions as it shows up in the tetrahedral molecular environment in ice, should be able to reproduce at least qualitatively the special properties of water. However, the achievement of quantitative agreement is much more difficult; e.g. the widely used ST2 as well as the TIPS2 [10] potentials yield a density maximum at about $25°C$.

A stringent test of the quality of interaction potentials is the calculation of collective properties like the shear viscosity η or the static dielectric constant ϵ_0.

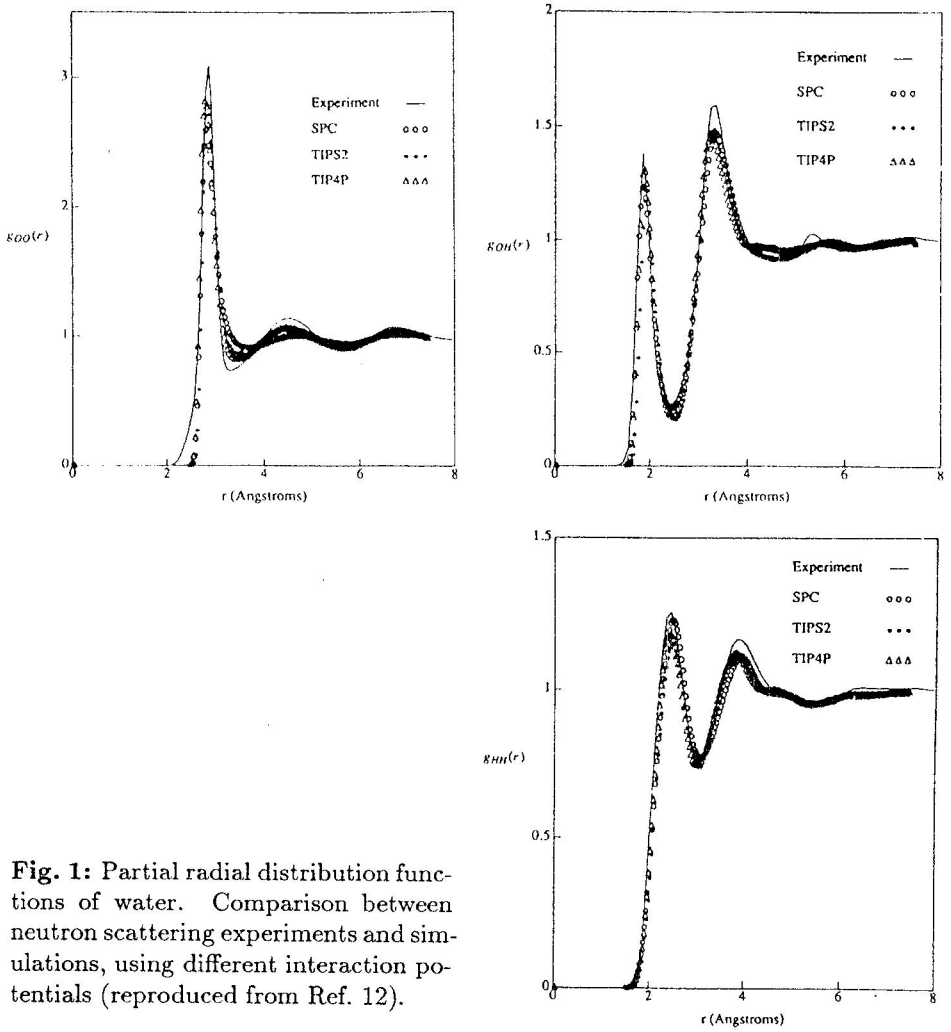

Fig. 1: Partial radial distribution functions of water. Comparison between neutron scattering experiments and simulations, using different interaction potentials (reproduced from Ref. 12).

Only recently, techniques have been developed to calculate ϵ_0 from the finite-size, periodic system of the MD simulations, although long-range orientational correlations are very important for this property.[13] It was shown that SPC and even more a 'flexible SPC' model, where intramolecular interactions had been added[14], could reproduce the experimental ϵ_0 satisfactory[12,15]. In contrast, the previously mentioned 4- or 5-site models yield larger deviations. Neumann[13] had pointed out that shifting the negative charge from the oxygen towards the hydrogens (as in MCY or TIPS2) decreases ϵ_0, whereas a shift in the other direction (as in ST2) increases ϵ_0. Thus SPC, the most simple model, where the negative point charge is located

on the oxygen seems to be also the 'best' effective pair potential, and moreover it is the 'cheapest' since it is 'fastest' with respect to computer time requirements, because it has only three distinct interaction sites. Unfortunately, even this model is not perfect; for example, it has been reported recently that the shear viscosity deviates by nearly a factor of two[16] from the experimentally known value.

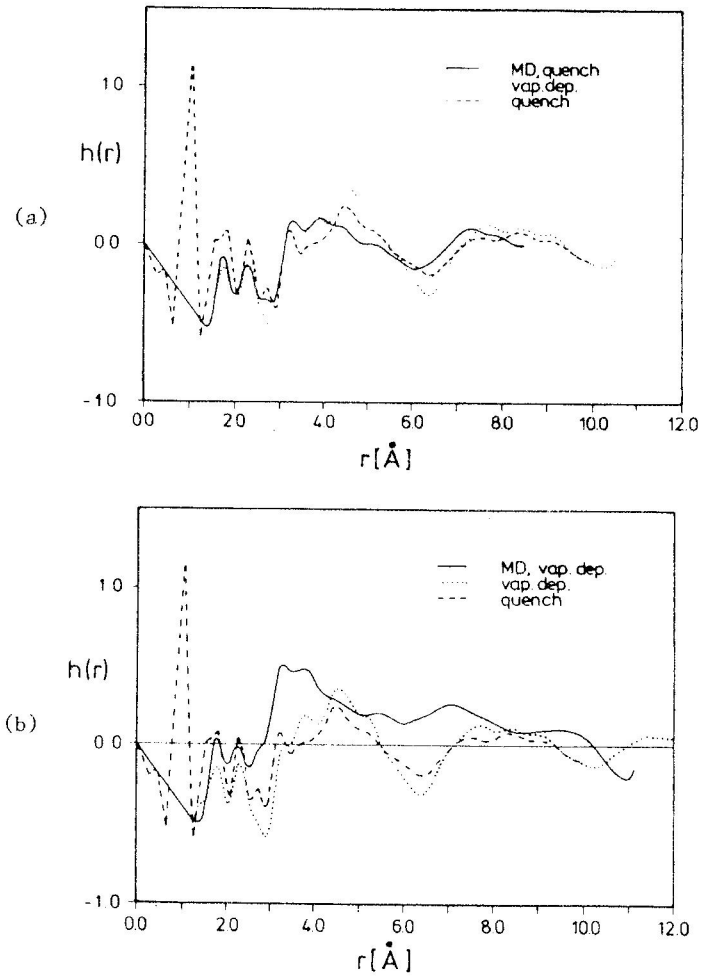

Fig. 2: Composite pair correlation functions of amorphous ice. Comparison of two experimental curves (dotted and dashed) with MD simulation results: (a) full line: rapid quench simulation and (b) full line: vapor deposition simulation.

The limits of applicability of an effective pair potential like SPC is also touched upon in a recent simulation of amorphous ice.[17] Figure 2a shows pair correlation functions

$$h(r) = 4\pi\rho r[g(r) - 1]$$

obtained from two independent neutron scattering experiments on low density amorphous ice (one sample was produced by vapor deposition,[18] the other by pressurizing crystalline ice[19]). $g(r)$ is the weighted sum of the partial pair correlation functions

$$g(r) = 0.092 g_{OO}(r) + 0.422 g_{OD}(r) + 0.486 g_{DD}(r),$$

as determined by the scattering power of the various nucleii (the neutron scattering lengths).[20]

The full line is from an MD simulation where the amorphous ice was produced by cooling the liquid rapidly. In view of the differences between the two experimental curves, the simulation results are reasonable. In contrast, Fig. 2b shows appreciable differences, when comparing with the results of an extended simulation of the vapor deposition process. It appears that the MD run produces a mixture of low- and high-density amorphous ice. One explanation is the fact that SPC is tailored to reproduce bulk water and is less well suited to model surfaces during a growth process. The same has been observed in simulations of amorphous silicon.

3. Hydration Effects

Knowledge of how molecular structures are hydrated is clearly of fundamental importance to molecular biology and solution chemistry. We now consider how the structure and dynamics of water is modified from the bulk behavior in the presence of both extended surfaces and isolated solute particles, as known from both experiments and computer simulations. There are countless detailed studies of the hydration of all kinds of solutes. Here we are interested in the description of some general effects and mechanisms. These studies, in fact, act as good examples of how simulations can provide the microscopic details of phenomena whose macroscopic effects are measured in experiments.

First consider an isolated spherical particle suspended in water. The particular ways in which the surrounding water structure may be modified can be envisioned in the following three ways, as sketched in Fig. 3.

(i) An uncharged sphere induces a hydrophobic hydration structure: from the point of view of the surrounding water, the uncharged particle essentially generates a water-excluding hole in the liquid. Energetically, it is unfavorable if the nearby water molecules are oriented so that many of their four tetrahedrally placed bonding "arms" (two proton donors and two acceptors) are directed toward this hole, since they would be left out of any bonding. Since the bonding arms are tetrahedrally placed, the bonding situation is optimized (for a sufficiently small particle) if one arm points directly away from the particle,

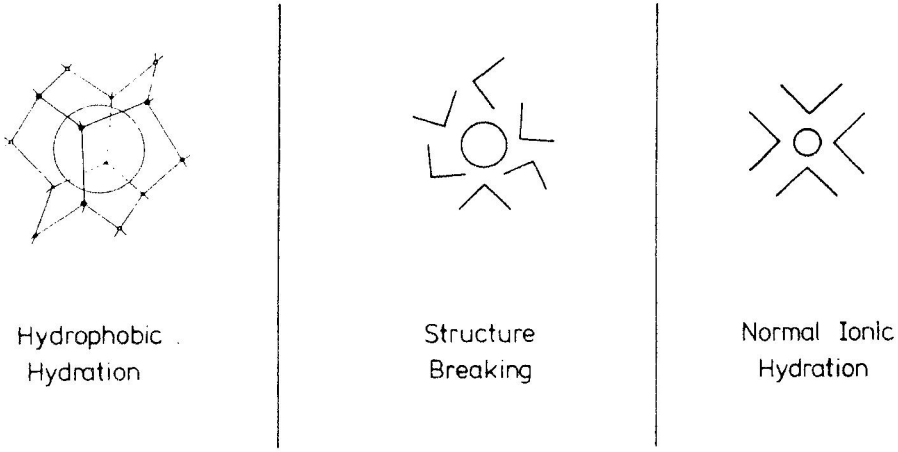

Fig. 3: Sketch of different hydration effects of simple spherical particles. From left to right the 'surface charge density' of the solute particle is increasing.

letting the other three bonds straddle the particle in a way that allows them to bond to similarly straddling water molecules nearby. Thus the neutral particle effectively repels H-bonding groups—this illustrates the name "hydrophobic" hydration. Moreover, such hydration structures are characterized by a strengthening of the water structure (comparable to a temperature decrease of a few K) and a corresponding reduction of the mobility of the molecules in the first hydration shell. An explanation for this observation will be given in the next chapter on stretched water.

(ii) Whereas the structure of the hydrophobic hydration shell is mainly due to the water-water interaction, in normal ionic hydration (e.g., around a Li^+-ion) a strong ion-water interaction is dominating, which leads to a pronounced orientational and translational ordering in the hydration shell, accompanied by a strong reduction of water mobility.

(iii) If the charge of the solute particle could be changed continuously, it should be possible to produce an arrangement where none of the two kinds of interactions is dominating, but rather balancing each other. It is easy to imagine that in this case there will be little order and even an increased mobility in the hydration shell. This is called the 'structure breaking effect.'

Such simple geometric ideas had been developed four decades ago on the basis of experimental observations on aqueous ionic solutions.[21,22] Although ionic charges can be varied continuously only in computer simulations, in real experiments, ionic radii can be changed in small steps. This variation of the 'surface charge density'

leads to different coulomb fields in the hydration shell. Focusing on the sequence Li^+, Na^+, through Cs^+ to larger univalent ions like the tetraalkylammonium ions $N(Alc)_4^+$, we pass from normal ionic hydration through structure breaking to hydrophobic hydration. And correspondingly the macroscopic viscosity as well as microscopic dynamic quantities like reorientation times or diffusion coefficients pass in this sequence a maximum of mobility between two extrema of immobilization.[22]

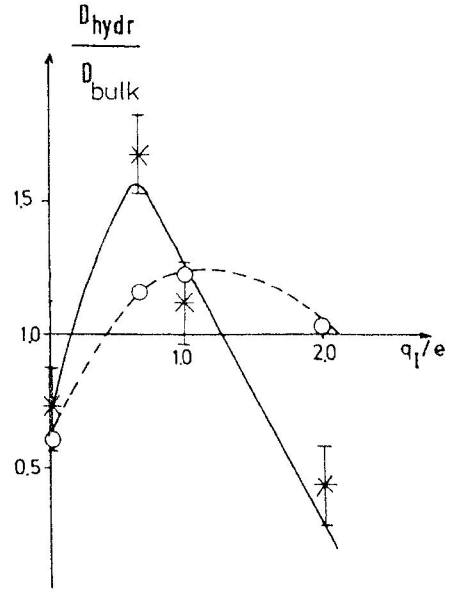

Fig. 4: Self diffusion coefficient in the first (full line) and second hydration shell (broken line) of particle with charge q.

In order to confirm the above mentioned microscopic interpretation of these experimental observations, computer simulations have proven useful. We discuss a simulation in which a Lennard-Jones sphere, with parameters matched to the physical properties of a xenon atom, is immersed in a system of 215 water molecules. Then, a variable charge q is included into the xenon force center. The system that results is one in which one can study the characteristics of hydration for a generic solute particle as a function of its charge[23]. The diffusion coefficient D of the water molecules in the first and second hydration shell was calculated as a measure of their mobility and is shown as a function of q in Fig. 4. The structural changes in the hydration shell can be understood by examining radial correlation functions. Figure 5 shows the O-H pair correlation function g_{OH} in the first hydration shell at three values of the ion charge q. The sharpness of the peaks in the g_{OH} function indicates the extent of well organized H-bonding. As one can see, the water structure, dominated by H-bonds is strongly distorted in the first hydration shell at high q. Figure 6 shows the pair correlation function g_{IO} for the ion itself with

the oxygen atoms of neighboring water molecules. The sharpness of the peaks here is a measure of the binding of the surrounding water molecules to the ion. As expected , the peaks are sharpest at larger values of q. These opposite trends create a maximum of disorder, slightly below $q = 1.0e$ (for the given particle size), as can be seen when studying orientation distribution functions.[23]

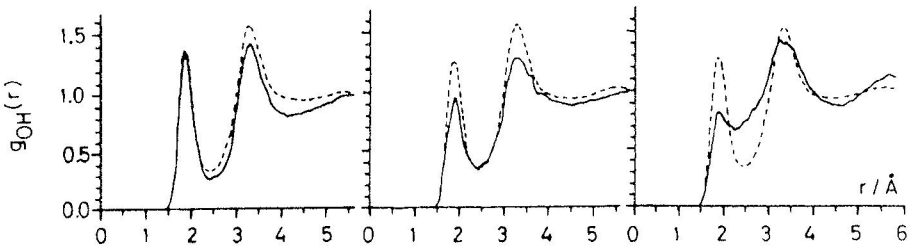

Fig. 5: Distortion of water structure in the first hydration shell with increasing charge ($q = 0, 1, 2e$, from left to right).

Summarizing, at low q the first hydration shell has a structure dominated by H-bonding, which results in low mobility of the molecules. As the charge increases, the H-bonded structure is destroyed by the Coulombic forces, producing a structure-breaking effect that increases the structural disorder and mobility. Eventually, however, the electrostatic forces become so strong so as to again decrease the mobility of the water molecules. In brief, the maximum in D versus q results from the competition between the two different types of structure that dominate hydration in the separate limits of vanishing q and increasing q; one dominated by H-bonding among water molecules, and the other by electrostatic bonding of the water molecules to the ion.

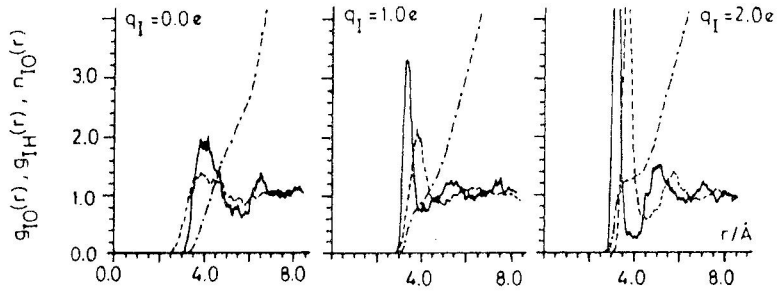

Fig. 6: Increasing ion-water correlation with increasing ionic charge.

The structure of water near extended surfaces takes in many of the concepts discussed above. For example, the structure of water near an electrically neutral surface is subject to the same energetic requirements as when near a neutral particle, with the result that again, water molecules do not tend to "waste" H-bonding groups by directing many of them toward the non-reactive surface. However, the result for an extended flat surface is different than that for a small particle: the surface can not be "straddled" by a tetrahedrally bonding water molecule, and so the optimal orientation requires one H-bonding group to point directly at the surface so that the other three can be angled upward toward other water molecules.[24]

The presence of a hydrophobic surface therefore tends to produce a well defined layer of water molecules next to it, imposing a thermally disturbed 'ice-like' orientational structure which propagates into the bulk for a few molecular layers before dying out. As with a charged particle, a charged surface subjects the nearby water structure to the competing effects of ordering due to the presence of the surface, and disordering due to H-bonds being overcome by electrostatic forces. And again, moderate changes in dynamic behavior (such as diffusion) as compared to bulk water, with sign and magnitude of the deviation depending on the particular interactions (including the smoothness of the surface), occur in the system.[25]

4. Structural Models and Stretched Water

There have been many attempts in the last decades to design simple structural models for water. A central feature of all of these is the assumed pattern formed by the hydrogen bonds between the water molecules.[26] The first MD simulations showed clearly that liquid water has to be considered as a 'defective continuous random network' of hydrogen bonds,[4,27] which is subject to a constant and rapid restructuring. Later it was shown that at any instance (and for any temperature) this network is spanning the whole system, i.e., that it exists well above its percolation threshold.[28] In accord with this picture, random bond percolation was an attempt by Stanley and Teixeira to model liquid water.[29] In this model, every site of a four-coordinated ice-lattice is considered to be occupied by a water molecule, and bonds are switched on randomly between nearest neighbor sites with a probability p_B that depends on the number of H-bonds in the system. This number is not a clear-cut value. Due to the continuous nature of the hydrogen-bond interaction, different definitions of an intact bond may be applied and depending on that, the total number of H-bonds as well as the bonding-probability p_B will vary. Most widespread is the use of an energetic definition, which considers a pair of water molecules as bonded if the interaction energy is below some negative cutoff value V_{HB}. In accord with the continuous nature of the H-bond interaction, V_{HB} may be varied such that p_B varies from 0 to 1, thus 'scanning' the connectivity pattern of a given water configuration by starting from very strong H-bonds and including weaker and weaker interactions.

With this approach one finds that distribution functions W_M which give the

weight fraction of water molecules belonging to finite nets of M molecules, as calculated from MD data, compare remarkably well with results predicted by percolation theory.[29,30] Motivated by the suggestion that the clustering of four-bonded water molecules is most important for the understanding of the unusual properties of supercooled water, [29] one may study the connectivity properties of the network by examining only those sites bonded to exactly four nearest neighbors. Although the *bonds* are still randomly distributed, the relevant sites, which consist now only of 4-bonded molecules, are *correlated*; hence one speaks of this more selective approach as *correlated site* percolation. One may then calculate probability distributions W_i^c for finding patches of i four-bonded molecules.

Although the agreement between the MD results and correlated site percolation theory seem striking at first glance,[29,30] one sees a systematic deviation in the results. This small difference

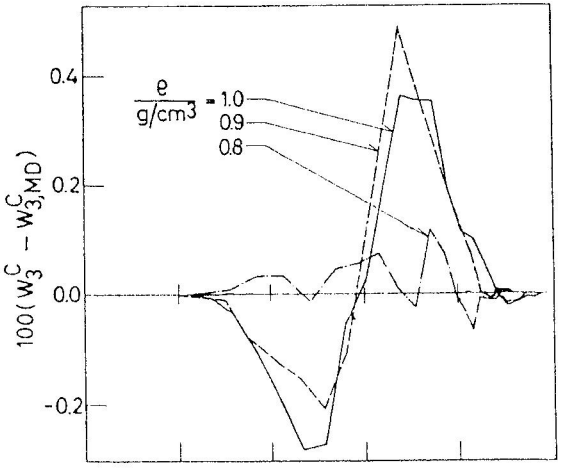

Fig. 7: Probability distribution for finding patches of 3 four-bonded molecules. Difference between percolation model and MD results. Abscissa: Bond probability p_B varies from 0 to 1.

$$\Delta W_i^c = W_{i_{perc}}^c - W_{i_{MD}}^c$$

is plotted in Fig. 7 as a function of p_B for the example $i = 3$ and for densities ranging from 1.0 to 0.8 g/cm^3. We see that the deviations vanish at 0.8 g/cm^3 for the whole range of p_B.

To understand why this is so, consider the MD results in Fig. 8. We see that with decreasing density water becomes *more* structured (at *constant* temperature of about 283K): the peaks and valleys of the pair correlation function g_{OH} become more pronounced. This is totally opposite to the behavior of 'normal' liquids, where a density decrease also *decreases* the structure. By integrating the first peak of g_{OO}, we can calculate the number of nearest neighbors. From Fig. 8b we see that for normal densities close to 1.0, a typical water molecule has an average of *more* than four molecules in its nearest neighbor shell, and only for densities at about 0.8 does the number of nearest neighbors approach four. Thus models which explicitly limit

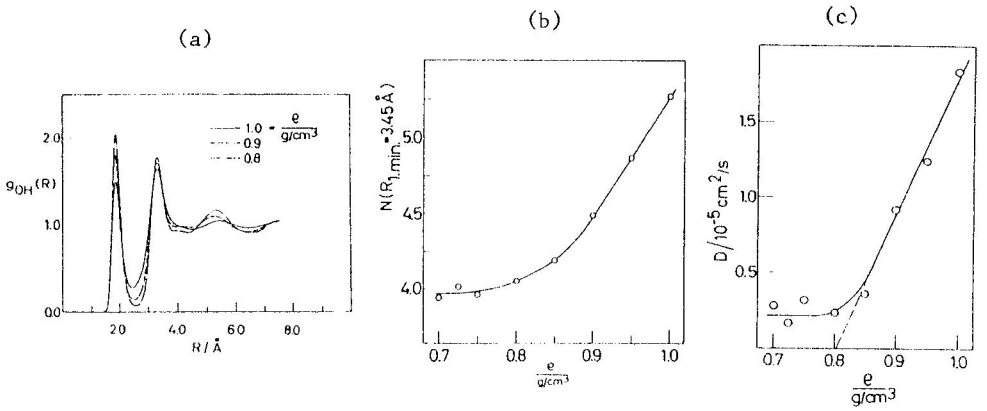

Fig. 8: Structure and microdynamics of stretched water. Density dependence of (a) OH-pair distribution function, (b) average number of neighbors, and (c) self-diffusion coefficient.

the maximum possible number of nearest neighbors to four cannot precisely mimic water at normal densities, but rather predict the structure of lower density water phases such as amorphous ice and stretched water.

Continuous random network (CRN) models were designed to describe disordered tetrahedral networks, as occurring in amorphous semiconductors,[31] but have also been largely applied to describe the structure of water and amorphous ice.[32] In fact, a remarkable agreement with the neutron scattering data on vapor deposited ice was reported.[20]

In Figs. 9 and 10 MD results for low density, stretched water are compared with an analysis of a typical CRN,[33] the Polk model, which is based on a 'ball-and-sticks' representation of a random network with exactly four nearest neighbors.[31] Figure 9 shows the average number $\langle N \rangle$ of faces of the Voronoi polyhedra (Wigner-Seitz cells for noncrystalline systems) constructed around each water molecule. Decreasing the density from 1.0 to 0.8 g/cm^3 the Polk model value (horizontal line) is approached, but not reached. Let SVP mean 'simplified Voronoi polyhedra', where all faces of 'indirect neighbors' are eliminated.[34] (For illustration, neighbor number 2 of the schematic drawing in Fig. 10 is such an indirect neighbor.) Figure 10 shows the oxygen radial distribution function of *direct* neighbors from SVP. The Polk model has two distinct peaks, which correspond to first and third neighbors. Again, the water distribution is approaching this form on decreasing density, but not at all reaching it. This shows that the real water network is distorted (even at 0.8 g/cm^3) compared to an 'ideal' CRN. This distortion extends beyond the first neighbor, as the surviving second peak indicates. This peak can be attributed to higher-order neighbors in a H-bond chain, which is strongly bent by the distortion of the network.

Although such deviations from an ideal CRN are quite substantial at larger

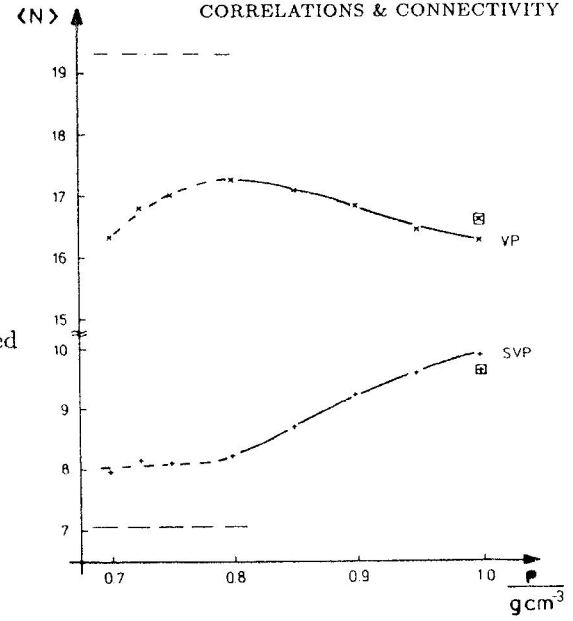

Fig. 9: Average number of faces of Voronoi and Simplified Voronoi polyhedra in stretched water. Horizontal lines: Polk model.

distances, most important for the water *dynamics* is the deviation from the *local* four-coordination. Figures 8b and 8c show a parallel decrease of the self-diffusion coefficient by nearly an order of magnitude, when the number of nearest neighbors is decreased from 5 to 4 by decreasing the global density.[35] This totally unusual behavior (in normal fluids the mobility is increased when the volume increases) can be explained by the following mechanism[36]: associated with the fifth neighbors are defects in the tetrahedral bond network ('bifurcated bonds') which offer paths with lower energy barriers between different network configurations and in turn enable the fast restructuring of the network with thermal energies kT much smaller than the hydrogen bond energies (a detailed description will be given in the next chapter by F. Sciortino).

Two important conclusions can be drawn:

(a) Network defects are important for the fluidity of water. Random network models which focus on tetrahedral local order without allowing arrangements of five nearest neighbors describe a gel-like, highly viscous water, as observed in the simulations of low density water.

(b) The above discussed findings offer a very simple mechanism for the occurrence of the Hydrophobic Hydration effect: The main effect of inert solutes is to lower *locally* the density of water and as a consequence the water is more structured and less mobile, as observed in stretched water.

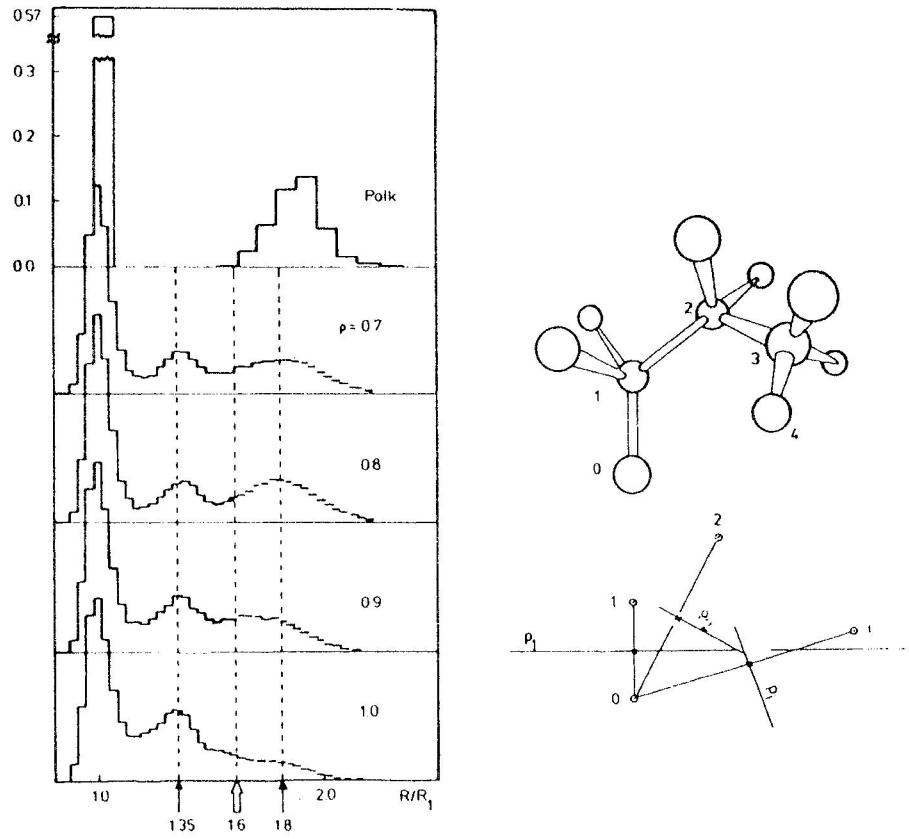

Fig. 10: Radial distribution function (oxygen positions) of direct neighbors (from simplified Voronoi polyhedra).

5. Conclusions

It has been speculated that the sometimes intriguing richness of the behavior of water as pure liquid and as solvent is the basis for the occurrence of life, offering evolution a wealth of possibilities to probe and exploit. The central role of the hydrogen-bond network has long been recognized, but only recently and largely due to contributions from computer simulations is our picture becoming less speculative and more quantitative. At the same time a few central mechanisms emerge, like the action of the fifth neighbors or the competition between hydrogen-bond forces and the influence of solutes. Moreover, the importance of metastable, particularly stretched water for the understanding of its possible role in biological membranes has been recognized.[37]

1. M. P. Allen and D. J. Tildesley, *Computer Simulation of Liquids* (Clarendon Press, Oxford, 1987).
2. J. L. Finney, J. E. Quinn, and J. O. Baum, in *Water Science Reviews*, Vol. 1, ed. F. Franks (Cambridge Univ. Press, 1985).
3. O. Matsuoko, E. Clementi, and M. Yoshimine, J. Chem. Phys. **64**, 1351 (1976).
4. A. Rahman and F. H. Stillinger, J. Chem. Phys. **55**, 3336 (1971); F. H. Stillinger and A. Rahman, J. Chem. Phys. **60**, 1545 (1974).
5. H. J. C. Berendsen, J. P. M. Postma, W. F. van Gunsteren, and J. Hermans, in *Intermolecular Forces*, ed. B. Pullman (Reidel, Dordrecht, 1981).
6. Ph. Bopp, in *The Physics and Chemistry of Aqueous Ionic Solutions*, eds. M. C. Bellissent-Funel and G. W. Neilson (Reidel, Dordrecht, 1987), and refs. therein.
7. P. Ahlström, A. Wallquist, S. Engström and Bo Jönsson, Mol. Phys. **68**, 563 (1989), and refs. therein
8. M. Sprik and M. L. Klein, J. Chem. Phys. **89**, 7556 (1988).
9. P. Cieplak, P. Kollmann and T. Lybrand, J. Chem. Phys. **92**, 6755 (1990).
10. W. L. Jorgensen, J. Chandrasekhar, J. D. Madura, R. W. Impey and M. L. Klein, J. Chem. Phys. **79**, 926 (1983).
11. M. Townsend, S. A. Rice and M. D. Morse, J. Chem. Phys. **79**, 2496 (1983).
12. H. J. Strauch and P. T. Cummings, Molec. Simulation **2**, 89 (1989).
13. M. Neumann, J. Chem. Phys. **85**, 1567 (1986), and refs. therein.
14. K. Toukan and A. Rahman, Phys. Rev. B **31**, 2643 (1985).
15. J. Anderson, J. I. Ullo and S. Yip, J. Chem. Phys. **87**, 1726 (1987).
16. P. T. Cummings and T. L. Varner, J. Chem. Phys. **89**, 6391 (1988).
17. U. Eßmann and A. Geiger, to be published.
18. M. R. Chowdhury, J. C. Dore, and J. T. Wenzel, J. Non-Cryst. Solids **53**, 247 (1982).
19. M. -C. Bellissent-Funel, J. Teixeira, and L. Bosio; J. Chem. Phys. **87**, 2231 (1987).
20. J. C. Dore, in *Water Science Reviews*, Vol. 1, ed. F. Franks (Cambridge University Press, 1985).
21. R. W. Gurney, *Ionic Processes in Solution* (McGraw Hill, New York, 1953); O. Y. Samoilov, Disc. Farad. Soc. **24**, 141 (1957).
22. G. Engel and H. G. Hertz, Ber. Bunsenges. Physik. Chemie **72**, 808 (1968).
23. A. Geiger, Ber. Bunsenges. Physik. Chemie **85**, 52 (1981).
24. C. Y. Lee, J. A. McCammon, and P. J. Rossky, J. Chem. Phys. **80**, 4448 (1984).
25. P. Linse, J. Chem. Phys. **90**, 4992 (1989), and refs. therein.
26. D. Eisenberg and W. Kanzmann, *The Structure and Properties of Water* (Clarendon Press, Oxford 1969).
27. F. H. Stillinger, Science **209**, 451 (1980).
28. A. Geiger, F. H. Stillinger, and A. Rahman, J. Chem. Phys. **70**, 4185 (1979).
29. H. E. Stanley and J. Teixeira, J. Chem. Phys. **73**, 3404 (1980); see also J. Teixeira's contribution in this book.
30. R. L. Blumberg, H. E. Stanley, A. Geiger, and P. Mausbach, J. Chem. Phys. **80**, 5230 (1984).
31. S. R. Elliott, *The Physics of Amorphous Materials* (Longman, London, 1983).
32. M. G. Sceats and S. A. Rice, in *Water, A Comprehensive Treatise*, Vol. 7, ed. F. Franks (Plenum, New York, 1982), p. 83.

33. N. N. Medvedev and A. Geiger, to be published.
34. N. N. Medvedev and Yu. I. Naberukhin, J. Structural Chem. **26**, 369 (1985).
35. A. Geiger, P. Mausbach and J. Schnitker, in *Water and Aqueous Solutions*, eds. G. W. Neilson and J. E. Enderby (A. Hilger, Bristol, 1986); A. Geiger and P. Mausbach, in *Hydrogen Bonded Liquids*, eds. J. C. Dore and J. Teixeira (Kluwer, Dordrecht, 1990).
36. F. Sciortino, A. Geiger, and H. E. Stanley, submitted.
37. P. M. Wiggins, Progr. Polymer Sci. **13**, 3 (1987).

Y.-C. ZHANG, AUSTEN ANGELL

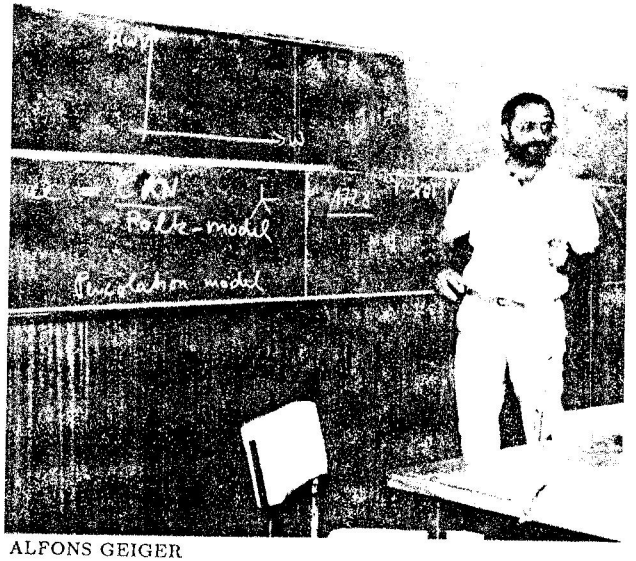

ALFONS GEIGER

JOHN DORE